Comparison of Infrared Laser Beam Shaping by Diffractive and Refractive Methods

Andrew Forbes[a], Anton du Plessis[b], Erich G. Rohwer[b]

[a]National Laser Centre, CSIR, PO Box 395, Pretoria 0001, South Africa;
[b]Laser Research Institute, University of Stellenbosch, Stellenbosch, South Africa

ABSTRACT

Infra-red laser beam shaping has the inherent difficulty that simple ray tracing methods often yield anomalous results, due primarily to the propagation effects at longer wavelengths. Techniques based on diffraction theory have been developed to overcome this, with associated parameters to determine when one approach is needed versus another. In this paper, infra-red (IR) beam shaping by diffractive methods is investigated and compared to refractive methods. Theoretical results on the beam shapers are calculated through a combination of analytical and numerical techniques, and using both ideal and non-ideal inputs. We show that the diffractive optical element (DOE) is remarkably resilient to input errors of wavelength and beam quality, while the refractive shaper is found to be difficult to model. Optical elements based on the two approaches were designed, and then fabricated from ZnSe. A comparison between the fabricated elements and the designed elements is presented, and some of the findings on practical problems in having such elements fabricated are highlighted.

Keywords: DOEs, refractive shaping, infra-red laser beams, beam propagation, beam shaping

1. INTRODUCTION

In refractive beam shaping, the bulk properties of optical components, such as thickness, surface curvature and refractive index cause the intensity and phase of an incoming laser beam to be changed. One could think of a lens as a beam shaper in this sense – the incident beam is transformed by refraction to generate a new outgoing beam. The advantage of this approach is that the system performance is fairly independent of wavelength, at least over a range where the refractive index does not vary significantly, thus permitting multiple beams (of different wavelengths) to be shaped with the same system, without loss of performance. The basic idea is very old (the first patent appeared roughly 30 yrs ago[1]), but has only recently[2] been resurrected with some improvements to the general concept. The popularity of this method is linked to the fact that the technology now exists to fabricate such elements. The method relies on a pair of aspheric elements arranged as either a Galilean or Keplerian system. The two aspheric lenses are designed so that the amplitude and phase of the incoming beam are converted to a new amplitude and phase after passing through both elements. The first aspheric is used for the amplitude conversion, while the second is used to control the phase of the outgoing beam. Present fabrication tolerances allow the design of the two aspheric surfaces to be realised in practice.

Diffractive beam shaping implies that the beam is passed through one or more elements where the feature sizes are small compared to the wavelength. By manipulating the phase of the incoming field, it can be transformed into a predetermined amplitude and phase in another plane. The advantage of this method in the IR over other wavelength regions is that diffractive elements for 10μm beams have fairly large feature sizes (due to the long wavelength), and therefore fabrication is possible. It also allows the design and fabrication of complex optical elements that can combine several functions into one (for example, shape as well as split a portion of the beam off). Although many design methodologies exist for diffractive beam shaping[3-8], in this paper we will consider an element based on the design method of Dickey[9]. In this method a Gaussian beam is passed through a diffractive element that converts the Gaussian to the Fourier transform of the desired shape. A transforming lens is then placed directly behind the element to take the

Laser Beam Shaping VI, edited by Fred M. Dickey, David L. Shealy, Proceedings of SPIE Vol. 5876
(SPIE, Bellingham, WA, 2005) · 0277-786X/05/$15 · doi: 10.1117/12.616654

inverse Fourier transform at the focal plane, which then returns the desired shape at this plane – in this case a beam with a flat-top intensity profile. By changing the lens, the parameters of the output field can be scaled.

At short wavelengths both techniques mentioned above have been shown to work. However, the wave nature of light becomes more pronounced as the wavelength increases. In the IR the propagation of laser beams can only be explained by considering wave arguments – simple ray tracing fails to accurately describe the salient features.

In the sections that follow we consider the advantages and disadvantages of designing beam shaping elements for use in the IR. We consider design and fabrication issues, and then show through simulation the expected behaviour of the elements. Finally, we propose an experiment to test the performance of these elements under ideal and non-ideal conditions, to verify the numerical predictions.

2. DESIGN AND FABRICATION

2.1 Beam Shapes

The beam shaping elements discussed in this paper convert Gaussian beams into Super-Gaussian or flat-top beams. The intensity (power density) profiles of these beams are defined as follows:

A Gaussian beam has an intensity function given by

$$I_g(r) = I_g \exp(-2(r/w_g)^2), \tag{1}$$

where w_g is the beam radius ($1/e^2$ value) and I_g is the peak intensity. Analytical expressions exist to propagate this type of field through any ABCD matrix system[10]. Gaussian beams have the property that their peak intensity is double their average intensity, and that the beam size w_g is already the second moment radius of this field.

A Super-Gaussian beam has an intensity function given by

$$I_s(r) = I_s \exp(-2(r/w_s)^{2p}), \tag{2}$$

where w_s is the beam radius (but not the second moment radius) and I_s is the peak intensity. Analytical expressions exist to propagate this type of field through any ABCD matrix system[11], but they are in general still numerically intensive. In the limit of large p, the Super-Gaussian "edges" become steeper, the peak intensity is equal to the average intensity, and the beam becomes a perfect flat-top. Due to energy conservation, the relationship between the peak values of the Gaussian and Super-Gaussian fields can be written as

$$I_s = \frac{2^{1/p} p w_g^2}{2 w_s^2 \Gamma(1/p)} I_g. \tag{3}$$

The lower peak intensity can be compensated for by decreasing the beam size relative to the Gaussian beam, but this has implications on the propagation of the field thereafter.

2.2 Design

The diffractive element was designed based on the method outlined by Dickey *et al.*[9], while the refractive shaper was designed following the method proposed by Hoffnagle *et al.*[2] In order to facilitate comparison, both beam shaping elements were designed for the same input beam parameters. The final design parameters are shown in table 1. The refractive design has the advantage of having tuneability across a wide range of wavelengths, and gives a flat wavefront out, which is ideal for further propagation. However, the output beam size is fixed, and can only be changed by imaging the output. The diffractive element is designed for one wavelength only (see numerical simulations for more on this point), and does not output a flat wavefront at the beam forming plane. However, it does allow for variable output beam sizes to be generated.

Table 1: Design parameters for the DOE and the refractive shaper.

PARAMETER	REFRACTIVE DESIGN	DIFFRACTIVE DESIGN
Input beam shape	Gaussian	Gaussian
Output beam shape	Super-Gaussian (p = 5)	Flat-top
Input beam size	7mm ($1/e^2$ value)	7mm ($1/e^2$ value)
Output beam size	10mm	Variable
Input wavelength	9 – 11μm	10.6μm
Input wavefront	Planar	Planar
Output wavefront	Planar	Free variable

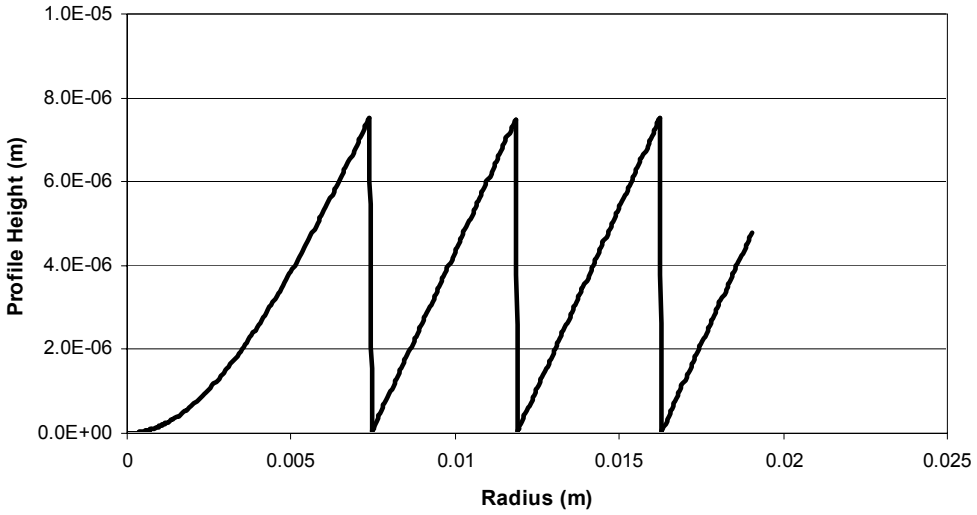

Figure 1: Calculated DOE height profile across a 19.05mm radius optic. The profile ranges from 0 to roughly 7.5μm in height, and is designed for a ZnSe substrate.

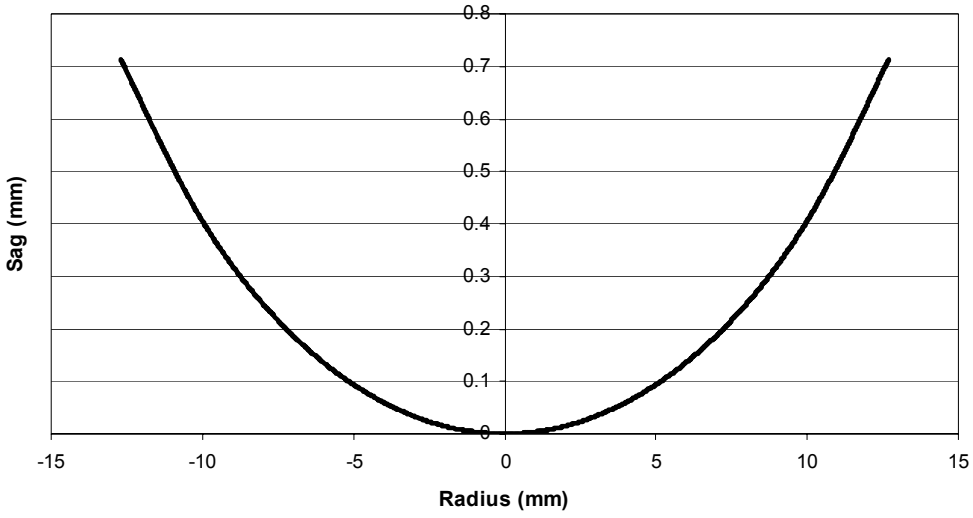

Figure 2: Sag of the second element across a 1" optic, showing characteristic aspherical nature.

2.3 Fabrication

All elements were fabricated by II-VI Inc. from 1.5" diameter ZnSe flat-flat optics, and were coated to ensure reflection losses were minimized at 10.6μm. Data for the fabrication was provided as a calculated height profile for the diffractive element, and as aspheric coefficients for the refractive elements. However, errors in the curve fitting to extract the latter coefficients, resulted in actual sag data used for the fabrication. Many of the conventional techniques for fabricating diffractive elements was found not to be suitable at this wavelength, due to the crystalline structure of many of the materials. All the salt based optics (e.g., KCl, KBr, NaCl etc) were considered too difficult to fabricate, while many fabricators mentioned inherent difficulties with ZnSe due to the variable rate of material removal in different directions in the crystal. Therefore, II-VI employed a diamond turning mechanism for the fabrication, which was considered suitable because of the larger feature sizes. The fabricate elements were tested using a Zygo surface interferometer, and the results are shown in figures 3 and 4.

Table 2: Comparison of designed and measured parameters for the DOE.

	Design	**Measured**
DOE Height Profile	7.56μm	~8.8μm
Zone 1 width	14.8mm	Could not be measured due to the range limitation of the
Zone 2 width	4.5mm	4.4mm
Zone 3 width	4.4mm	4.2mm

Using the Zygo data one can compare the design to the fabricated element (see Table 2). Clearly the zone spacings are consistent with the design, and the transitions of the zones are of good quality (see figures 3 and 4). However, the zone heights show deviations from the design. Recalling that the zone spacing determines the function of the element, and the height the wavelength for which it is suited, the deviation in height implies an optimal operating wavelength other than the design of 10.6μm (assuming a constant refractive index, a wavelength closer to 12μm would now be ideal).

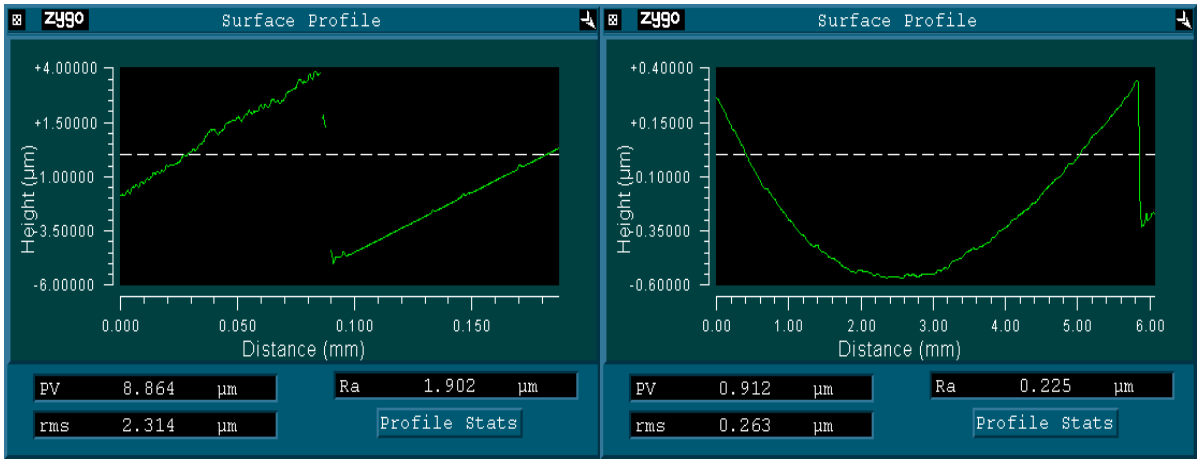

Figure 3: Surface profiles across the DOE, showing a zoomed view of one of the zone transitions (left graphic) and the full central region (right graphic); the height scale is X10 on the central region plot. The Zygo data suggests the zone heights are roughly 8.8µm, whereas the design was for roughly 7.5µm.

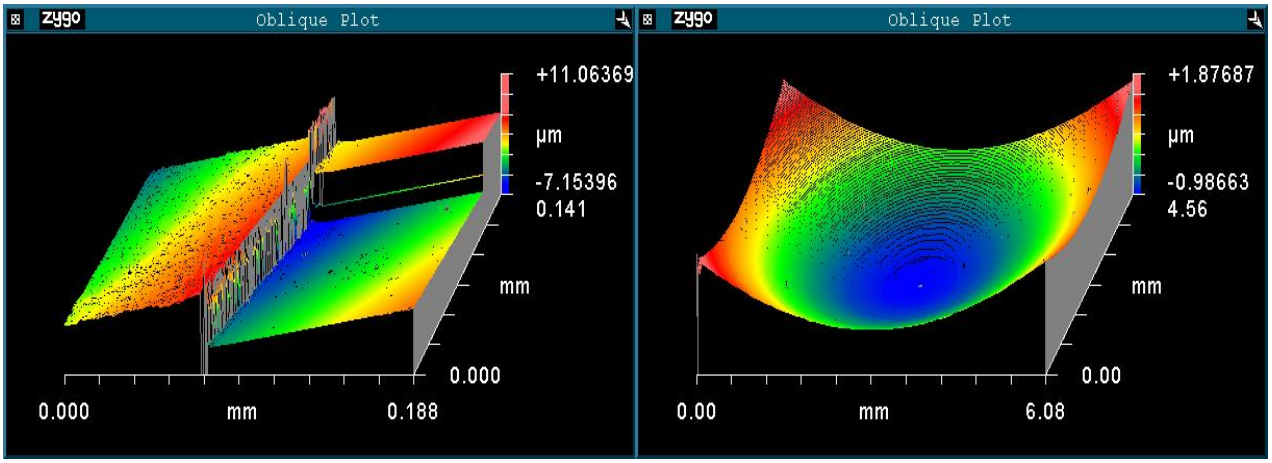

Figure 4: 3D plots of the surface structure of the DOE, with the left graphic showing the surface across a zone transition, and the right graphic showing the central phase region. The zone transition is well defined and shows no measurable slope error.

3. NUMERICAL SIMULATIONS

Many numerical techniques exist for evaluating diffractive elements in general[8,12], while only some aspects of this particular design method have been considered[8,9]. What has not previously been considered are practical issues such as wavelength tuneability, input beam quality, and errors in the placement of the element along the propagation axis of the incoming beam (which can contribute to both beam size and input phase errors). Radial offsets and beam size errors have been considered elsewhere[12], and are consistent with results generated as part of this study previously[13].

In the case of the refractive shaper, most simulations that were attempted in GLAD (commercial physical optics software package) for the IR failed. This could be due to the programme, or our use of it, but we suspect rather that this is due to the fact that the ray tracing methods cannot correctly predict the wave nature of light, which is important when the design

wavelength is at such long wavelengths[14], a point already considered in some refractive design methods[15]. To illustrate the problem, consider the following simple scenario: an incident beam with its waist on the lens is focused to a new waist some distance away. Since the wavefront at the lens is flat, a ray based argument would suggest that the rays entering the lens are therefore parallel, implying that the new waist location should be exactly at the focal plane of the lens. However, a wave based view yields the correct result: that the new waist is found at a position given by

$$z_0 = \frac{f}{1+\left(\frac{fM^2\lambda}{\pi w_0^2}\right)^2}, \tag{4}$$

where M^2 is the laser beam quality factor, f is the focal length of the lens, and w_0 is the beam radius on the lens. One can interpret this as follows – even though the wavefront at the lens is flat, the information of the inherent divergence of the beam cannot be ignored. In refractive beam shaping methods, such aspects simply cannot be incorporated into the design. However, these effects become less significant as the wavelength of the light becomes small ($\lambda \to 0$), and at an infinitely small wavelength (perfect ray), the waist is again found at the focal plane of the lens, and the ray tracing methods will be exact. The discrepancies shown here pose some questions as to the validity of refractive design approaches for the IR.

3.1 Wavelength dependence

3.1.1 Refractive design

The refractive design has the advantage of use across a range of wavelengths, and the method predicts wavelength tuneability by simply changing the separation distance between the elements (designed for a separation of 150mm at a wavelength of 10.6μm). The dependence of the separation distance between the elements on wavelength, $d(\lambda)$, is given by[2]

$$d(\lambda) = d_0 \frac{n_0 - 1}{n(\lambda) - 1}, \tag{5}$$

with n the refractive index, and the subscript 0 indicating the designed parameter. Using information on the refractive index of ZnSe at different wavelengths[16], the wavelength tuneability is shown in figure 5. The design predicts that by changing the separation between the elements by as little as 1mm, one can tune across the entire CO_2 laser wavelength range without any loss of resulting beam shape quality.

3.1.1 Diffractive design

The required phase profile of the DOE is created in a substrate by etching out a specific height profile in the material. In most diffractive based designs the height of the element determines the design wavelength, while the zone spacing determines the function of the element. The relationship between the DOE height and the net phase change experienced by the laser beam on passing through the element is given by:

$$\Delta\phi = \frac{2\pi}{\lambda}(n-1)h \cdot \tag{6}$$

Consequently, errors in the performance of the element are introduced when operated at wavelengths other than the design wavelength. The performance of the DOE was tested using design and non-design wavelengths in the CO_2 laser tuneability range, and the results are shown in figure 6. The design wavelength is shown together with two wavelengths in the 9μm branch of the CO_2 lasing lines. The three flat-top beams are for all practical purposes indistinguishable from one another. This is a surprising result, and may be a function of this specific element. Nevertheless, such a result has not been suggested for this design method before.

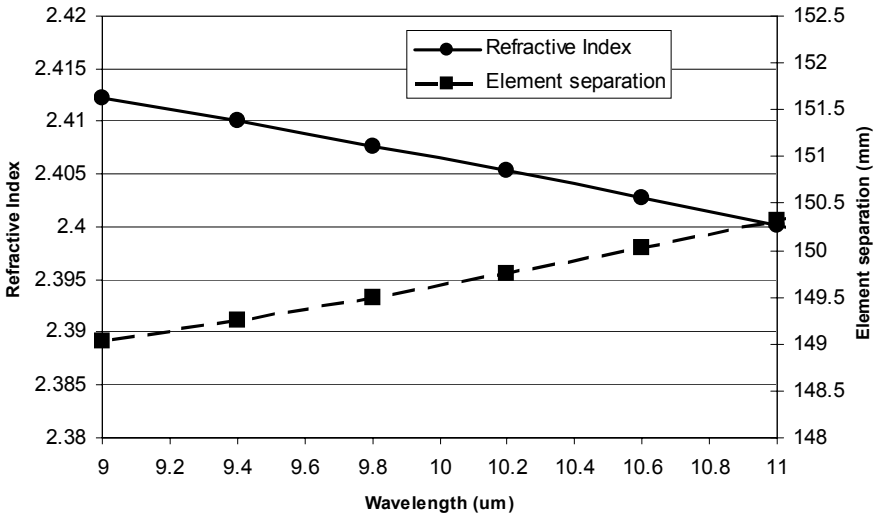

Figure 5: Plot of the refractive index of ZnSe and the resulting element separation needed for wavelength tuneability, across the 9 – 11 μm wavelength band of line tunable CO_2 lasers.

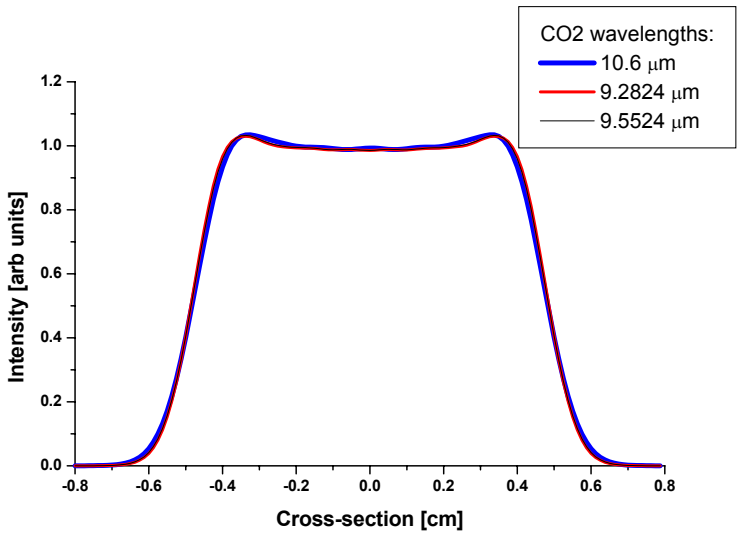

Figure 6: Simulated performance of the DOE at the design wavelength (10.6μm) and two non-design wavelengths (~9.3μm and ~9.6μm). The resulting beam shape is very close to the ideal flat-top, but the distances at which the shapes are generated differ.

3.2 Beam quality dependence

CO_2 laser beams (transverse profiles) are rarely purely Gaussian, and often have some higher order modes mixed with the TEM_{00} mode. It is not unusual for CO_2 laser beams to operate with M^2 values in the 1–1.5 range (i.e., from excellent Gaussians to mixtures of modes). In particular, a typical TEA laser will have an M^2~1 in the confined direction (perpendicular to the electrodes), while having an M^2~1.5 in the free direction (gas flow direction). Understanding how the DOE will perform when the beam quality is not what one expects is therefore important if the DOE is to be used with "real" lasers. The beam quality aspect outlined here has two main contributions to errors when considering the input beam to the DOE: (a) a change in the laser beam profile (however small) from the ideal Gaussian, and (b) a change in the wavefront and beam size experienced by the DOE due to slightly different propagation effects from the laser to the DOE. These potential errors are simulated for the DOE.

3.2.1 Input beam profile dependence

To model the impact of this potential problem on the performance of the DOE, a "mixed" beam was introduced, consisting of a combination of TEM_{01}, and a "donut" mode made from a combination of TEM_{10} and TEM_{00} modes. The mix was created using 1 part of the donut mode (combination of the TEM_{01} and TEM_{10}), with *n* parts (referred to as the mixture value) of the TEM_{00} mode. This beam was propagated through the DOE and the resulting beam shape investigated.

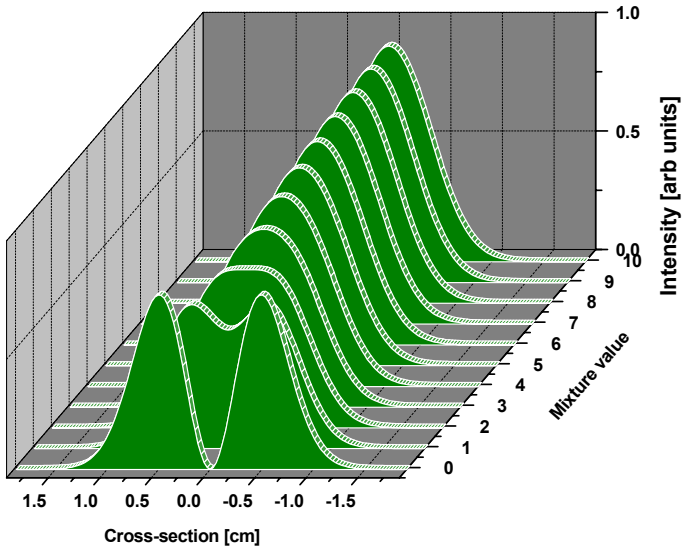

Figure 7: Input beam to the beam shaper as a function of the mixture value n, i.e., *n* = 10 implies 10 parts TEM_{00} and 1 part donut mode.

The results are summarized in Figures 7 and 8. In Figure 7 the initial input beam to the DOE is shown as a function of the mixture value (*n*). When *n* = 10 the beam is very nearly Gaussian (M^2 ~ 1.2 for this case), while for *n* = 0, the beam is a pure donut (non-Gaussian). From Figure 8 we can see that the DOE does not perform well when the input beam deviates significantly from Gaussian. However, the resulting profiles are considered only at the designed transforming plane. If one considers the propagation of the field after the DOE towards the transforming plane, then a different picture emerges. Figure 9 shows the results for the *n* = 10 case, over a propagation distance of 3m (shown from 1m onwards).

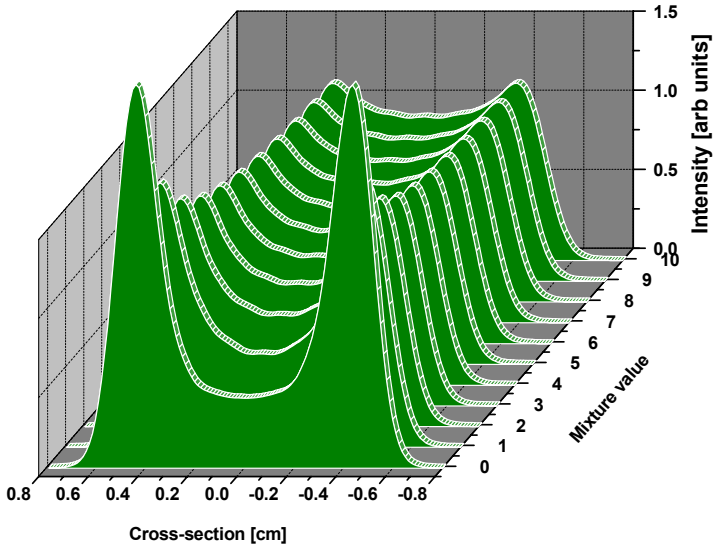

Figure 8: Final beam shape at the focal plane of the transforming lens, as a function of the mixture value n. As expected, the DOE is not very tolerant to deviations from the design case of a pure Gaussian input, but does give acceptable results for small amounts of the higher order mode.

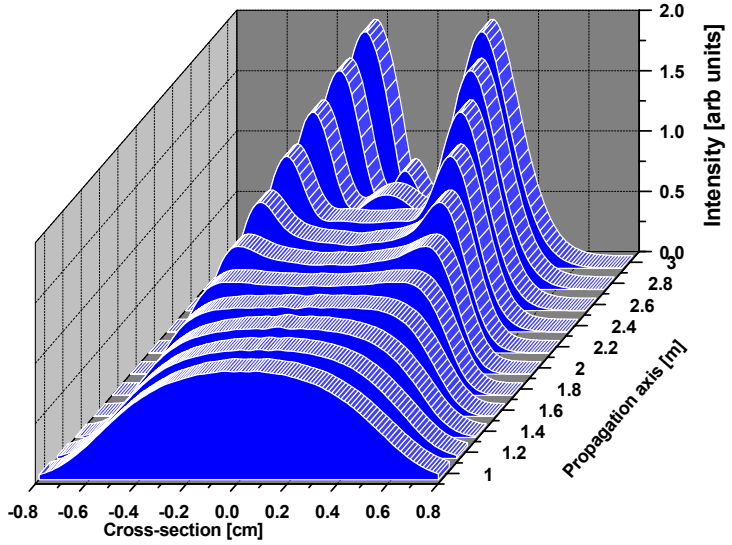

Figure 9: Propagation after the DOE of a non-ideal input beam profile. The DOE still creates a flat-top beam, but at a target plane closer than the design, as with a smaller final output beam.

The design point is at roughly 2m, but from the propagation analysis it is clear that the flat-top is in fact generated closer to the DOE, at a distance of between 1.6m and 1.8m from the DOE, and is slightly smaller than the designed size. Thus the impact of poor beam quality on performance as shown in Figure 8 can be largely negated if one works at a transform plane closer to the DOE, and is prepared to accept small deviations in actual flat-top size.

3.2.2 Axial offset dependence

In practice it is not always possible to position the DOE at precisely the waist position of the beam, and therefore errors can be introduced due to an axial offset, Δz, as measured along the direction of propagation of the incoming Gaussian beam. This error can also be due to propagation effects whereby the waist of the laser beam is slightly moved due to a different beam quality factor from the laser output. An offset error such as this will change both the size and the phase of the beam incident on the DOE. The results for the design case of a 7mm waist is shown in figure 10.

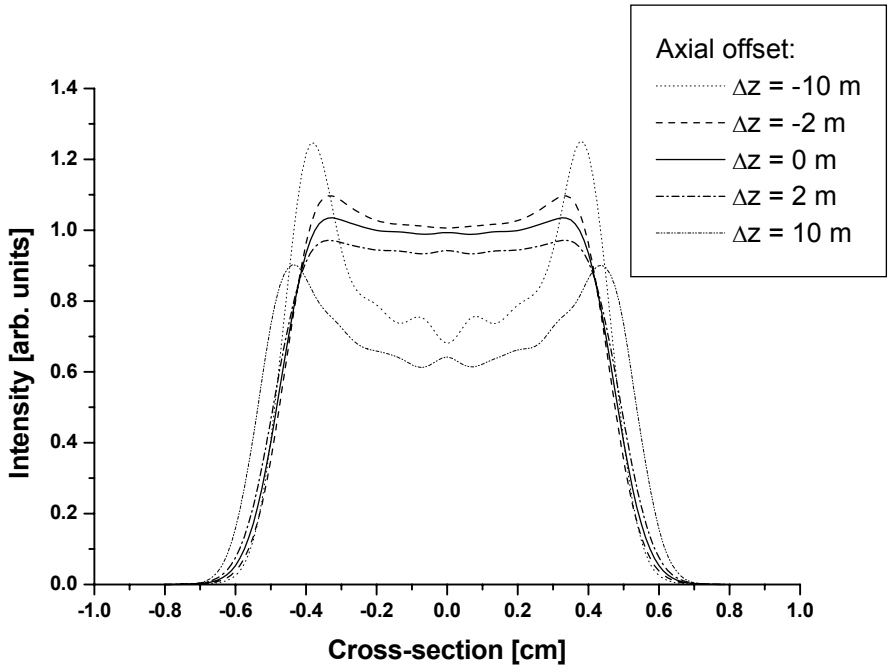

Figure 10: Change in beam shape due to a shift along the propagation axis of the beam. This could be due to an alignment error, or due to propagation errors.

Within reasonable limits, the axial offset does not influence the beam shape appreciably, and only becomes significant at large offset values.

4. FUTURE EXPERIMENTS

An experiment has been established to test the predictions put forward in this paper, with the results to be presented on completion. However, an outline of the experiment is given here for the interested reader. An Edinburgh Instruments cw PL-2 laser (CO_2 laser) was used as the laser source. The resonator was comprised of a grating at one end and a R=3m output coupler at the other, separated by a length of 75cm (roughly 45cm gain length). The grating allowed line tuneability across the 9 – 11μm wavelength range. An Optical Engineering spectrum analyzer was used to determine the operating wavelength, while a Coherent LM-45 detector was used to measure the cw power output (typically up to a maximum of 4W was measured). The measured beam quality from the laser showed an $M^2 = 1$, but varied slightly from day to day due to small misalignments within the resonator, reaching a maximum of 1.43. This makes it suitable for testing the beam quality predictions made earlier.

The required 7mm waist of the Gaussian beam was generated by various focusing mirrors and an adjustable telescope made from a combination of a f = – 50mm and a f = 100mm lens, with a micrometer adjustable separation. This system proved to be very sensitive to changes in the beam quality from the laser, and is in general labour intensive. The beam shaping optics were placed in the region of the 7mm beam waist. The refractive elements were micrometer mounted for fine adjustments to the separation distance between the elements. In the case of the DOE, practical requirements meant that the transforming lens was placed a short distance from the DOE instead of the ideal scenario of no separation between them. Results from these experiments will be presented at a later stage.

5. CONCLUSION

We have designed and fabricated beam shaping optics for the IR by both refractive and diffractive methods. The diffractive element has been modeled numerically to determine its properties under various input conditions. In particular, errors due to input wavelength and beam quality have been investigated, and it was shown that the DOE element is remarkably resilient under these non-ideal conditions. This suggests that this design method is suitable for implementation of elements with "real" laser systems – i.e., systems where the laser beam is not always the ideal, as long as it is possible to work closer than the design plane.

The refractive shaper does not lend itself to easy simulation by the means just discussed. There is no way to describe beam quality in terms of rays – this and other considerations have led the authors to question the validity of the refractive beam shaping method for long wavelengths (far IR). Experiments have started to test the concepts and predictions contained in this paper.

ACKNOWLEDGEMENTS

We would like to thank Mr P. Neethling and Mr S. Ntenteni for general assistance and Ms T. Baisitse for help with the Zygo analysis.

REFERENCES

1. J.L. Kreuzer, "Coherent light optical system yielding an output beam of desired intensity distribution at a desired equiphase surface", US Patent 3476463, 1969.
2. J.A. Hoffnagle, C.M. Jefferson, "Design and performance of a refractive optical system that converts a Gaussian to a flattop beam", *Applied Optics*, **39** (30), pp. 5488-5499, 2000.
3. P.A. Belanger and C. Pare, "Optical resonators using graded-phase mirrors", *Optics Letters*, **16** (14), 1991.

4. C. Pare, P.A. Belanger, “Custom laser resonators using graded-phase mirrors”, *IEEE Journal of Quantum Electronics*, **28** (1), 1992.
5. R. Hocke, M. Collischon, “Line selective resonators with variable reflectivity gratings (VRG) for slab-laser geometry”, *Proc. SPIE*, **3930**, 2000.
6. U.D. Zeitner, F. Wyrowski, H. Zellmer, “External Design Freedom for Optimization of Resonator Originated Beam Shaping”, *IEEE J. Quantum Electron*., **36**, pp.1105-1109, 2000.
7. U.D. Zeitner, H. Aagedal, F. Wyrowski, “Comparison of resonator-originated and external beam shaping”, *Appl. Opt*., **38**, pp.980-986, 1999.
8. F.M. Dickey, S.C. Holswade “Laser Beam Shaping – Theory and Techniques”, Marcel Dekker (New York), 2000.
9. F.M. Dickey, S.C. Holswade, “Gaussian laser beam profile shaping”, *Opt. Eng*., **35** (11), pp.3285-3295, 1996.
10. A. Yariv, “Quantum Electronics”, John Wiley and Sons (New York), pp. 116-129, 1989.
11. F. Gori, “Flattened Gaussian beams”, *Optics Communications*, **107**, pp 335-341, 1994.
12. Y. Danziger, E. Hasman, A.A. Friesem, A.W. Lohmann, “Multilevel diffractive elements for generalized wavefront shaping”, *Opt. Eng.,* **35** (9), pp. 2556-2565, 1996.
13. A. du Plessis, “A charactrisation of beam shaping devices and a tunable Raman laser”, MSc dissertation (University of Stellenbosch), 2002.
14. M. Born, E. Wolf, “Principles of Optics”, Cambridge University Press (Cambridge), 1999.
15. R. Estrela Llopis, J.A. Ramos de Campos, J. Sochacki, “Phase retardation for Gaussian beam homogenizer: geometrical design and its verification” *Proc. SPIE,* **2870**, pp. 417-425, 1996.
16. Commercially published data: Advanced Materials Division, BDH Limited, England.